


RESEARCH ARTICLE

# Model-free adaptive robust control based on TDE for robot with disturbance and input saturation

Xia Liu , Lu Wang and Yong Yang

School of Electrical Engineering and Electronic Information, Xihua University, Chengdu 610039, China

**Corresponding author:** Xia Liu; Email: [xliucd@163.com](mailto:xliucd@163.com)

**Received:** 31 March 2023; **Revised:** 4 July 2023; **Accepted:** 13 July 2023; **First published online:** 10 August 2023

**Keywords:** nonlinear robot; unknown dynamics and disturbance; input saturation; time delay estimation; adaptive robust control

## Abstract

A model-free adaptive robust control based on time delay estimation (TDE) is proposed for robot in the presence of disturbance and input saturation. TDE is utilized to estimate the complicated nonlinear terms of the robot including unknown dynamics and disturbance, and a TDE error observer is developed to estimate the inevitable TDE error. When the input torque of the robot exceeds the upper or lower limit of the input saturation, an auxiliary system and a saturation deviation boundary adaptive law are employed to mitigate the negative impact of input saturation on the position tracking. Finally, the robust control law is obtained by backstepping. The stability of the closed-loop system is proved by Lyapunov functions, and the validity of the proposed method is demonstrated by comparative simulations and experiments. Compared with the model-based controllers and other model-free controllers, the proposed method does not necessitate the accurate dynamic model of the complicated system and with lower computation. Moreover, it can guarantee the desired position tracking performance of the robot even subject to disturbance and input saturation simultaneously.

## 1. Introduction

The robot has extensive usage in a variety of fields, including industry, underwater exploration, and rehabilitation medicine [1–3]. However, the robot is usually of substantial nonlinearities, coupled dynamics, and model uncertainty. Moreover, the systems often suffer from disturbance due to unknown environments and external uncertainties. Therefore, a variety of control schemes have been proposed to accurately control the robots.

The control schemes for robot subjected to disturbance can be generally divided into two categories: model-based control and model-free control [4]. Thereinto, model-based control necessitates complicated calculations of the accurate dynamic model, such as sliding mode control [5–7] and model predictive control (MPC) [8–10]. Whereas, model-free control does not rely on the dynamic model so that it can be applied to the situations where the model of the system is difficult to compute or unknown. In ref. [11], an attack detection approach was proposed for DC servo motor systems, which did not require the prior knowledge of the system model. In refs. [12, 13], fuzzy control techniques were employed to approximate the system model. In refs. [14–17], neural network control techniques were adopted to learn the system model. However, fuzzy control and neural network control require a large number of adjustable parameters and high computational burden. In addition, model-free control can also be achieved through adaptive control technique which can be broadly categorized into learning-based adaptive control [18] and non-learning-based adaptive control [19]. Nevertheless, adaptive control also requires extensive computation and may converge slowly for highly complicated and unknown system.

As an effective and relatively simple model-free method, which is easy to implement, and is robust to estimate the unknown uncertain system's model, time delay estimation (TDE) has been extensively

investigated and applied in the control of robot. The fundamental idea of TDE is to estimate the complicated dynamics and external disturbance at the current instant using the time delay information at the previous sampling instant [20]. A variety of TDE-based control strategies for nonlinear robot systems with uncertainty and unknown disturbance have been proposed. For uncertain robots with external disturbance and backlash hysteresis, a robust model-free control method combining TDE and adaptive terminal sliding mode was proposed in ref. [21]. Through TDE this method does not necessitate prior knowledge of unknown backlash hysteresis and system dynamics. In the case of nonlinear underactuation, an artificial-delay control approach with adaptive gains was developed in ref. [22]. This approach does not rely on linearity, the structure of the mass matrix, the boundedness of state derivatives, or unactuated states. A backstepping approach combined with TDE for exoskeleton robot adaptive control was proposed in ref. [23] to estimate the unknown dynamics and address the external bounded disturbance. Although refs. [20–23] can achieve model-free control with TDE. However, if the robot is exposed to significant external disturbance, the effectiveness of TDE declines and the TDE error increases, which will severely affect the control performance of the system [24].

To effectively compensate for the TDE error, a model-free adaptive sliding mode control was proposed in ref. [25] for robot with uncertainty, and an adaptive law based on sliding mode was developed to lessen the TDE error. In ref. [26], an adaptive robust control was proposed for robot. This control enabled chattering-free, high precision, and strong robustness by combining TDE with adaptive integral sliding mode. In ref. [27], a robust controller using fractional-order nonsingular terminal sliding modes was developed to enhance the position tracking performance of the robot. A nonlinear adaptive law was developed for the TDE control gain to suppress TDE error. In ref. [28], the estimation error of TDE was regarded as a disturbance, and an adaptive sliding mode observer was developed to estimate the TDE error. Although TDE error can be effectively suppressed with the methods in refs. [25–28], when the robot is subjected to significant external disturbance or the state error increases, not only TDE error appears in the systems, but an overlarge control torque may also appear for maintaining the tracking performance, which can cause the required control input torque to rapidly reach saturation [29–31].

The deviation between the actual input saturation control torque and the controller command input torque is called input saturation deviation. In robot trajectory tracking control, the input saturation deviation needs to be specially considered, otherwise the system performance may deteriorate, and even the system stability is destroyed [32, 33]. In ref. [34], a method employing active disturbance rejection control and predefined tracking performance functions was proposed. It dealt with the position tracking control of robot manipulators in the presence of input saturation and uncertainty. However, the method in ref. [34] is only for one-DOF link robot manipulators. In ref. [35], an offline model predictive control based on a linear parameter variation model was proposed for free-floating space robots. The input saturation problem was addressed in the constraints of the model predictive control. In ref. [36], a new fractional sliding control method was proposed for a spherical robot. In order to handle input saturation, an auxiliary system was introduced. In ref. [37], a robust adaptive tracking control approach was proposed for multi-input multi-output mechanical systems with unknown disturbance under actuator input saturation. Thereinto, an actuator saturation compensator was introduced to attenuate the adverse effects of actuator saturation. However, all the methods in refs. [35–37] depend on the system model and necessitate prior knowledge about complicated system dynamics.

In this paper, a model-free adaptive robust control method based on TDE is proposed for trajectory tracking of uncertain robot with disturbance and input saturation. The primary contributions of this paper are as follows:

- Unlike other model-free controllers, TDE is used to approximate the nonlinear dynamics of the robot with disturbance and input saturation with lower computation. Thus, the proposed method is model-free, which does not necessitate the accurate dynamic model of the complicated system.
- A TDE error observer is developed to compensate for the TDE error. Thus, the inherent TDE error is reduced so that the nonlinear terms can be approximated more accurately.

- Compared with ref. [37], an auxiliary system is constructed by the deviation boundary between the command control input and the actual control input subject to input saturation, and an adaptive law is developed for the saturation deviation boundary. Hence, the adverse effects of input saturation can further be diminished.
- Different from ref. [23], the final control law is developed by backstepping with the TDE, the TDE error observer, the auxiliary system, and the saturation deviation boundary adaptive law. Hence, the proposed method is robust to disturbance and input saturation simultaneously.

### 2. Dynamic model of robot

The dynamic model of a robot with  $n$ -degrees of freedom ( $n$ -DOF) is

$$M(q)\ddot{q} + C(q, \dot{q})\dot{q} + G(q) + F(\dot{q}) = u + d \tag{1}$$

where  $q, \dot{q}, \ddot{q} \in \mathbf{R}^{n \times 1}$  are the angular position, angular velocity, and the angular acceleration of the joints, respectively,  $M(q) \in \mathbf{R}^{n \times n}$  is the symmetric positive definite inertia matrix,  $C(q, \dot{q}) \in \mathbf{R}^{n \times n}$  is the vector of the Coriolis and centrifugal term,  $G(q) \in \mathbf{R}^{n \times 1}$  is the gravity,  $F(\dot{q}) \in \mathbf{R}^{n \times 1}$  is the joint friction force,  $d \in \mathbf{R}^{n \times 1}$  is the disturbance, and  $u \in \mathbf{R}^{n \times 1}$  is the actual control torque.

The actual control torque  $u$  is limited by input saturation, that is,  $u = \text{sat}(\tau)$ ,  $\tau \in \mathbf{R}^{n \times 1}$  is the command control input for the controller, saturation function is  $\text{sat}(\tau_i) = \begin{cases} \text{sign}(\tau_i) * v_i, & |\tau_i| \geq v_i \\ \tau_i, & |\tau_i| < v_i \end{cases}$ ,  $v_i > 0$  is a constant,  $\text{sign}(\bullet)$  is the symbolic function, and the subscript  $i = 1, 2, \dots, n$  indicates the  $i$ -th joint of the robot.

Let  $x_1 = q, x_2 = \dot{q}$ , then the dynamic model (1) can be transformed into the following state-space equation as:

$$\begin{cases} \dot{x}_1 = x_2 \\ \dot{x}_2 = M^{-1}(q) \text{sat}(\tau) + M^{-1}(q) (-C(q, \dot{q})\dot{q} - G(q) - F(\dot{q}) + d) \\ y = x_1 \end{cases} \tag{2}$$

where  $y$  is the output of the robot. Notice that the nonlinear term  $M^{-1}(q) \text{sat}(\tau) + M^{-1}(q)(-C(q, \dot{q})\dot{q} - G(q) - F(\dot{q}) + d)$  in Eq. (2) includes input saturation and all the uncertainty terms of the robot such as disturbance, and uncertain dynamics.

### 3. TDE

In practice, it is hard to acquire the dynamic model (2) due to the unknown disturbance and dynamics in the nonlinear terms. TDE technique can estimate all the nonlinear terms of robot at the current instant using the torques and accelerations of the system output at the previous sampling instant.

By introducing a positive definite diagonal constant matrix  $\bar{M}$ , Eq. (2) can be rewritten as:

$$\begin{cases} \dot{x}_1 = x_2 \\ \dot{x}_2 = \bar{M}^{-1} \text{sat}(\tau) - \bar{M}^{-1} S_n \\ y = x_1 \end{cases} \tag{3}$$

where  $S_n = ((M(q) - \bar{M})\ddot{q} + C(q, \dot{q})\dot{q} + G(q) + F(\dot{q}) - d)$  concentrates all the uncertain terms and unknown disturbance in the nonlinear terms of the robot dynamics. Hence, we employed TDE to estimate  $S_n$ , which contains all the uncertain terms and unknown disturbance of the robot under input saturation.

The second equation in Eq. (3) can be rewritten as:

$$S_n = u - \bar{M}\dot{x}_2 \tag{4}$$

Define  $\hat{S}_n$  as the estimation of  $S_n$ , then we have

$$S_n \approx \hat{S}_n = S_{n(t-L)} = u_{t-L} - \bar{M}\dot{x}_{2(t-L)} \tag{5}$$

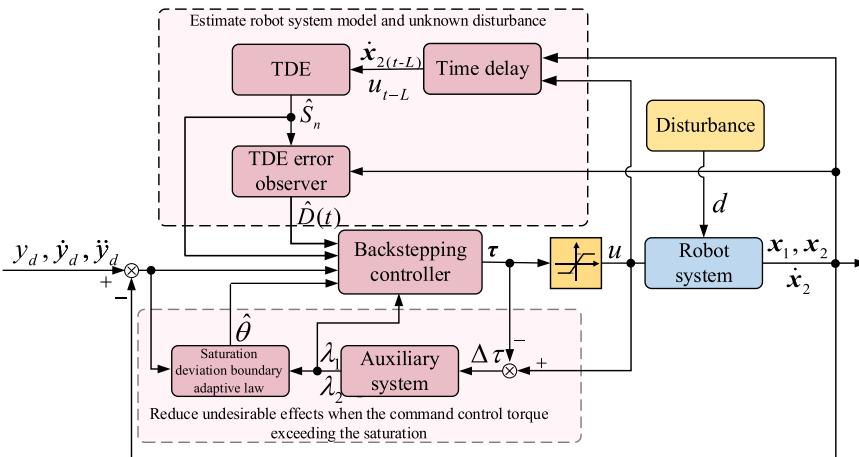


Figure 1. System control block diagram.

where  $L$  is the delayed time, which is usually set as a sampling time in practice, and  $\dot{x}_{2(t-L)}$  represents the value of  $\dot{x}_2$  after time delay.

Then the TDE error can be obtained as:

$$\boldsymbol{\varepsilon} = S_n - \hat{S}_n \tag{6}$$

Substituting Eqs. (5) and (6) into Eq. (3), we can obtain

$$\begin{cases} \dot{x}_1 = x_2 \\ \dot{x}_2 = \bar{M}^{-1} u - \bar{M}^{-1} (u_{t-L} - \bar{M} \dot{x}_{2(t-L)} + \boldsymbol{\varepsilon}) \\ y = x_1 \end{cases} \tag{7}$$

Notice that the position  $x_1$  is available. The velocity  $x_2$  and acceleration  $\dot{x}_2$  can be calculated by  $x_1$  as follows:

$$x_2(t) = \frac{x_1(t) - x_1(t-L)}{L} \tag{8}$$

$$\dot{x}_2(t) = \frac{x_1(t) - 2x_1(t-L) + x_1(t-2L)}{L} \tag{9}$$

**Lemma 1** ([38, 39]). *If the gain matrix  $\bar{M}$  satisfies the following condition:*

$$\|I - M^{-1}(q)\bar{M}\| < 1 \tag{10}$$

*then the TDE error  $\boldsymbol{\varepsilon}$  is bounded, that is,  $\|\boldsymbol{\varepsilon}\| \leq \vartheta_1$ , where  $\vartheta_1$  is a positive constant and  $I$  denotes the unit matrix with proper dimension.*

#### 4. Model-free adaptive robust control based on TDE

The block diagram of the model-free adaptive robust control based on TDE for robot with disturbance and input saturation is shown in Fig. 1. It consists of three main parts. The first part is the TDE and the TDE error observer which is to estimate the dynamic model and the unknown disturbance of the robot to obtain the model-free characteristics. The second part includes the auxiliary system and the saturation deviation boundary adaptive law which is to reduce the undesirable effects when the control torque exceeds the input saturation. The last part contains a backstepping controller which lumps the output results of the above two parts to obtain the final model-free adaptive robust control. The control goal is to achieve desired position tracking despite the unknown disturbance and input saturation.

4.1. TDE error observer

Since TDE uses the output value of the previous sampling instant to approximately estimate the nonlinear terms at the current instant. When the robot is subject to significant external disturbance, the output value of the previous sampling instant may have error which will affect the system performance or even cause system instability. Thus, a TDE error observer is introduced to observe the TDE error and compensate for the TDE error so that the nonlinear terms can be approximated more accurately.

The second equation in Eq. (7) can be rewritten as:

$$\dot{x}_2 = \bar{M}^{-1}u - \bar{M}^{-1}(u_{t-L} - \bar{M}\dot{x}_{2(t-L)}) + D(t) \tag{11}$$

where  $D(t) = -\bar{M}^{-1}\epsilon$ . Since  $\bar{M}$  is a constant matrix, then according to Lemma 1, we know that  $\|\epsilon\| \leq \vartheta_1$  in  $D(t)$ . Thus, there exist two positive constants  $\vartheta_2$  and  $\vartheta_3$ , such that  $\|D(t)\| \leq \vartheta_2$  and  $\|\dot{D}(t)\| \leq \vartheta_3$ .

Then the TDE error can be represented in the form as:

$$D(t) = -(\bar{M}^{-1}u - \bar{M}^{-1}u_{t-L} + \dot{x}_{2(t-L)}) \tag{12}$$

Now, the TDE error observer is developed as:

$$\begin{cases} \hat{D}(t) = z + Jx_2 \\ \dot{z} = -Jz - J(\bar{M}^{-1}u - \bar{M}^{-1}u_{t-L} + \dot{x}_{2(t-L)} + Jx_2) \end{cases} \tag{13}$$

where  $\hat{D}(t)$  is the observed value of  $D(t)$ ,  $z$  is the state of the TDE error observer, and  $J$  as a diagonal matrix is the gain of the observer and satisfies  $J - \frac{1}{2}I > 0$ .

**Lemma 2** ([40]). (Rayleigh–Ritz Theorem) *The Hermitian matrix  $H$  and the vector  $\varpi$  satisfy the following inequality:*

$$\lambda_{\min}(H)\|\varpi\|^2 \leq \varpi^T H \varpi \leq \lambda_{\max}(H)\|\varpi\|^2 \tag{14}$$

where  $\lambda_{\min}(\bullet)$  and  $\lambda_{\max}(\bullet)$  denote the minimum eigenvalue and the maximum eigenvalue of the matrix, respectively.

**Theorem 1.** *Consider the robot (7) is subject to external disturbance, if the TDE error observer (13) is employed to estimate the TDE error  $D(t)$  in Eq. (11), then the TDE error observer estimation error  $\tilde{D}(t) = D(t) - \hat{D}(t)$  will be asymptotically stable in  $\Omega = \{\tilde{D}(t): \|\tilde{D}(t)\| \leq \vartheta_3/\lambda_{\min}(J)\}$ .*

**Proof.** Differentiating  $\hat{D}(t)$  and substituting Eqs. (11) and (13) into it one can obtain

$$\begin{aligned} \dot{\tilde{D}}(t) &= \dot{z} + J\dot{x}_2 = -Jz - J(\bar{M}^{-1}u - \bar{M}^{-1}u_{t-L} + \dot{x}_{2(t-L)} + Jx_2) + J\dot{x}_2 \\ &= -Jz - JJx_2 + JD(t) = -J\hat{D}(t) + JD(t) \\ &= J\tilde{D}(t) \end{aligned} \tag{15}$$

Define the Lyapunov function as:

$$V_D = \frac{1}{2}\tilde{D}(t)^T \tilde{D}(t) \tag{16}$$

Substituting Eq. (15) into the derivative of Eq. (16) and applying Lemma 2 yield

$$\begin{aligned} \dot{V}_D &= \tilde{D}(t)^T (\dot{D}(t) - J\tilde{D}(t)) \\ &\leq \|\tilde{D}(t)\| \vartheta_3 - \|\tilde{D}(t)\|^2 \lambda_{\min}(J) \\ &\leq -\|\tilde{D}(t)\| \left( \lambda_{\min}(J) \|\tilde{D}(t)\| - \vartheta_3 \right) \end{aligned} \tag{17}$$

Form Eq. (17), if  $J$  is properly selected which satisfies  $\|\tilde{D}(t)\| > \vartheta_3/\lambda_{\min}(J)$ , then we have  $\dot{V}_D < 0$ . Therefore, the TDE error observer is asymptotically stable to an any small  $\Omega$ . Theorem 1 is proved.  $\square$

### 4.2. Input saturation auxiliary system

In practice, the command control torques of the controller are sometimes limited by the input saturation. When the command control torques exceed, the saturation will result in position tracking error, which will degrade the system performance and even destroy the system stability. To reduce the negative effects of input saturation, the following auxiliary system is further constructed based on ref. [37] by introducing the saturation deviation boundary:

$$\begin{cases} \dot{\lambda}_1 = -p_1\lambda_1 + \lambda_2 \\ \dot{\lambda}_2 = \bar{M}^{-1}(-p_2\lambda_2 + \Delta\tau) - \lambda_2 \left\| \bar{M}^{-1} \right\|^2 \|\Delta\tau\|^2 \end{cases} \quad (18)$$

where  $\lambda_1 \in \mathbf{R}^{n \times 1}$ ,  $\lambda_2 \in \mathbf{R}^{n \times 1}$  are the states of the auxiliary system, and  $p_1, p_2$  are positive definite constant gain matrixes. Also,  $\Delta\tau = \text{sat}(\tau) - \tau$  is the input saturation deviation which represents the deviation between the actual control input and the command control input under the input saturation limit. Thus, Eq. (11) can be rewritten as:

$$\dot{x}_2 = \bar{M}^{-1}\tau + \bar{M}^{-1}\Delta\tau - \bar{M}^{-1}(u_{t-L} - \bar{M}\dot{x}_{2(t-L)}) + \hat{D}(t) \quad (19)$$

**Remark 1.** The input saturation should still ensure the controllability of the robot in practice. Thus, it is generally assumed that  $\Delta\tau$  is bounded and there exists a constant  $\theta > 0$  satisfying  $\|\Delta\tau\|^2 \leq \theta$ .

### 4.3. Backstepping controller

The estimated output of the TDE, the TDE error observer, and the auxiliary system are lumped into the backstepping controller. A saturation deviation boundary adaptive law and a model-free adaptive robust controller are developed. Thereby, the robot can track the desired position even with unknown disturbance and input saturation.

**Lemma 3** ([41]). (Young’s inequality) For  $\forall a, b \geq 0, A > 1, B > 1$  and  $\frac{1}{A} + \frac{1}{B} = 1$ , then

$$ab \leq \frac{a^A}{A} + \frac{b^B}{B} \quad (20)$$

**Lemma 4** ([42]). If there exists a positive definite and first-order derivative continuous Lyapunov function  $V(x)$  satisfying  $\Phi_1(\|x\|) \leq V(x) \leq \Phi_2(\|x\|)$ , such that  $\dot{V}(x) \leq -\rho V(x) + \Lambda$ , then  $x(t)$  is uniformly bounded, where  $\Phi_1, \Phi_2$  are  $K$ -class functions and  $\rho, \Lambda$  are positive constants.

**Step 1.** Define two error variables as:

$$\begin{cases} e_1 = x_1 - y_d - \lambda_1 \\ e_2 = x_2 - \alpha - \lambda_2 \end{cases} \quad (21)$$

where  $y_d$  is the desired position and  $\alpha$  is the virtual control input to the robot system.

Differentiating  $e_1$  in Eq. (21) and substituting it into Eq. (18), we can obtain

$$\dot{e}_1 = e_2 + \alpha - p_1\lambda_1 \quad (22)$$

Consider the Lyapunov function as:

$$V_1 = \frac{1}{2}e_1^T e_1 \quad (23)$$

Differentiating  $V_1$  and combining with Eq. (22) yields

$$\dot{V}_1 = e_1^T (e_2 + \alpha + p_1\lambda_1 - \dot{y}_d) \quad (24)$$

Based on Eq. (24), the following virtual control input is selected as:

$$\alpha = -K_1 e_1 + \dot{y}_d - p_1\lambda_1 \quad (25)$$

where  $\mathbf{K}_1$  is a positive definite constant matrix. Then, substituting Eq. (24) into Eq. (23) yields

$$\dot{\mathbf{V}}_1 = \mathbf{e}_1^T \mathbf{e}_2 - \mathbf{e}_1^T \mathbf{K}_1 \mathbf{e}_1 \tag{26}$$

**Step 2.** Consider the Lyapunov function as:

$$\mathbf{V}_2 = \mathbf{V}_1 + \frac{1}{2} \mathbf{e}_2^T \mathbf{e}_2 \tag{27}$$

From Eqs. (19) and (21), differentiating  $\mathbf{e}_2$  in Eq. (21), we have

$$\begin{aligned} \dot{\mathbf{e}}_2 &= \bar{\mathbf{M}}^{-1} \boldsymbol{\tau} - \bar{\mathbf{M}}^{-1} (\mathbf{u}_{t-L} - \bar{\mathbf{M}} \dot{\mathbf{x}}_{2(t-L)}) + \hat{\mathbf{D}}(t) - \dot{\boldsymbol{\alpha}} \\ &\quad + \bar{\mathbf{M}}^{-1} \mathbf{p}_2 \lambda_2 + \lambda_2 \left\| \bar{\mathbf{M}}^{-1} \right\|^2 \|\Delta \boldsymbol{\tau}\|^2 \end{aligned} \tag{28}$$

Differentiating  $\mathbf{V}_2$  and combining with Eq. (28), it can be obtained that

$$\begin{aligned} \dot{\mathbf{V}}_2 &= \dot{\mathbf{V}}_1 + \mathbf{e}_2^T \left( \bar{\mathbf{M}}^{-1} \boldsymbol{\tau} - \bar{\mathbf{M}}^{-1} (\mathbf{u}_{t-L} - \bar{\mathbf{M}} \dot{\mathbf{x}}_{2(t-L)}) + \hat{\mathbf{D}}(t) - \dot{\boldsymbol{\alpha}} \right. \\ &\quad \left. + \bar{\mathbf{M}}^{-1} \mathbf{p}_2 \lambda_2 + \lambda_2 \left\| \bar{\mathbf{M}}^{-1} \right\|^2 \|\Delta \boldsymbol{\tau}\|^2 \right) \\ &\leq \mathbf{e}_1^T \mathbf{e}_2 - \mathbf{e}_1^T \mathbf{K}_1 \mathbf{e}_1 + \mathbf{e}_2^T \left( \bar{\mathbf{M}}^{-1} \boldsymbol{\tau} - \bar{\mathbf{M}}^{-1} (\mathbf{u}_{t-L} - \bar{\mathbf{M}} \dot{\mathbf{x}}_{2(t-L)}) \right. \\ &\quad \left. + \hat{\mathbf{D}}(t) - \dot{\boldsymbol{\alpha}} + \bar{\mathbf{M}}^{-1} \mathbf{p}_2 \lambda_2 + \lambda_2 \left\| \bar{\mathbf{M}}^{-1} \right\|^2 \mu \boldsymbol{\theta} \right) \end{aligned} \tag{29}$$

where  $0 < \mu < 1$ .

Then the model-free adaptive robust controller  $\boldsymbol{\tau}$  can be developed as:

$$\begin{aligned} \boldsymbol{\tau} &= \mathbf{u}_{t-L} - \mathbf{p}_2 \lambda_2 + \bar{\mathbf{M}} \left( -\mathbf{K}_2 \mathbf{e}_2 - \mathbf{e}_1 - \hat{\mathbf{D}}(t) + \dot{\boldsymbol{\alpha}} - \dot{\mathbf{x}}_{2(t-L)} \right. \\ &\quad \left. + \Xi \lambda_2 \left\| \bar{\mathbf{M}}^{-1} \right\|^2 \mu \hat{\boldsymbol{\theta}} \right) \end{aligned} \tag{30}$$

where  $\Xi = \text{diag}[\text{sign}(\mathbf{e}_{2i})]$ ,  $\mathbf{K}_2$  is a positive definite constant matrix and  $\hat{\boldsymbol{\theta}}$  is the estimation of  $\boldsymbol{\theta}$ .

Since  $\|\Delta \boldsymbol{\tau}\|^2 \leq \theta$ , we can get

$$\mathbf{e}_2^T \lambda_2 \left\| \bar{\mathbf{M}}^{-1} \right\|^2 \|\Delta \boldsymbol{\tau}\|^2 \leq \sum_{j=1}^n |e_{2j}| \|\lambda_{2j}\| \left\| \bar{\mathbf{M}}^{-1} \right\|^2 \mu \boldsymbol{\theta} \tag{31}$$

$$\mathbf{e}_2^T \Xi \lambda_2 \left\| \bar{\mathbf{M}}^{-1} \right\|^2 \mu \hat{\boldsymbol{\theta}} = \sum_{j=1}^n |e_{2j}| \|\lambda_{2j}\| \left\| \bar{\mathbf{M}}^{-1} \right\|^2 \mu \hat{\boldsymbol{\theta}} \tag{32}$$

Substituting Eq. (30) into Eq. (29) yields

$$\begin{aligned} \dot{\mathbf{V}}_2 &\leq \mathbf{e}_1^T \mathbf{e}_2 - \mathbf{e}_1^T \mathbf{K}_1 \mathbf{e}_1 + \mathbf{e}_2^T \left( \bar{\mathbf{M}}^{-1} \boldsymbol{\tau} - \bar{\mathbf{M}}^{-1} \mathbf{u}_{t-L} - \bar{\mathbf{M}} \dot{\mathbf{x}}_{2(t-L)} \right. \\ &\quad \left. + \hat{\mathbf{D}}(t) - \dot{\boldsymbol{\alpha}} + \bar{\mathbf{M}}^{-1} \mathbf{p}_2 \lambda_2 + \lambda_2 \left\| \bar{\mathbf{M}}^{-1} \right\|^2 \|\Delta \boldsymbol{\tau}\|^2 \right) \\ &= \mathbf{e}_1^T \mathbf{e}_2 - \mathbf{e}_1^T \mathbf{K}_1 \mathbf{e}_1 + \mathbf{e}_2^T \left( \bar{\mathbf{M}}^{-1} \mathbf{u}_{t-L} - \bar{\mathbf{M}}^{-1} \mathbf{p}_2 \lambda_2 \right. \\ &\quad \left. - \Xi \lambda_2 \left\| \bar{\mathbf{M}}^{-1} \right\|^2 \mu \hat{\boldsymbol{\theta}} - \mathbf{K}_2 \mathbf{e}_2 - \mathbf{e}_1 - \hat{\mathbf{D}}(t) \right. \\ &\quad \left. + \dot{\boldsymbol{\alpha}} - \dot{\mathbf{x}}_{2(t-L)} - \bar{\mathbf{M}}^{-1} \mathbf{u}_{t-L} + \dot{\mathbf{x}}_{2(t-L)} + \hat{\mathbf{D}}(t) - \dot{\boldsymbol{\alpha}} \right. \\ &\quad \left. + \bar{\mathbf{M}}^{-1} \mathbf{p}_2 \lambda_2 + \lambda_2 \left\| \bar{\mathbf{M}}^{-1} \right\|^2 \|\Delta \boldsymbol{\tau}\|^2 \right) \end{aligned}$$

$$\begin{aligned}
 &= -\mathbf{e}_1^T \mathbf{K}_1 \mathbf{e}_1 - \mathbf{e}_2^T \mathbf{K}_2 \mathbf{e}_2 + \mathbf{e}_2^T \left( -\Xi \lambda_2 \left\| \bar{\mathbf{M}}^{-1} \right\|^2 \mu \hat{\boldsymbol{\theta}} \right. \\
 &\quad \left. + \lambda_2 \left\| \bar{\mathbf{M}}^{-1} \right\|^2 \|\Delta \boldsymbol{\tau}\|^2 \right)
 \end{aligned} \tag{33}$$

Substituting Eqs. (31) and (32) into Eq. (33) yields

$$\begin{aligned}
 \dot{V}_2 &\leq -\mathbf{e}_1^T \mathbf{K}_1 \mathbf{e}_1 - \mathbf{e}_2^T \mathbf{K}_2 \mathbf{e}_2 - \sum_{j=1}^n |e_{2j}| \|\lambda_{2j}\| \left\| \bar{\mathbf{M}}^{-1} \right\|^2 \mu \hat{\boldsymbol{\theta}} \\
 &\quad + \sum_{j=1}^n |e_{2j}| \|\lambda_{2j}\| \left\| \bar{\mathbf{M}}^{-1} \right\|^2 \mu \boldsymbol{\theta} \\
 &= -\mathbf{e}_1^T \mathbf{K}_1 \mathbf{e}_1 - \mathbf{e}_2^T \mathbf{K}_2 \mathbf{e}_2 - \sum_{j=1}^n |e_{2j}| \|\lambda_{2j}\| \left\| \bar{\mathbf{M}}^{-1} \right\|^2 \mu \tilde{\boldsymbol{\theta}}
 \end{aligned} \tag{34}$$

where  $\tilde{\boldsymbol{\theta}} = \hat{\boldsymbol{\theta}} - \boldsymbol{\theta}$ .

**Step 3.** Consider the Lyapunov function as:

$$V = V_2 + \frac{1}{2\mu} \tilde{\boldsymbol{\theta}}^T \tilde{\boldsymbol{\theta}} + \frac{1}{2} \tilde{\mathbf{D}}(t)^T \tilde{\mathbf{D}}(t) + \frac{1}{2} \lambda_1^T \lambda_1 + \frac{1}{2} \lambda_2^T \lambda_2 \tag{35}$$

Differentiating Eq. (35) and using Lemma 3 and Eq. (34) lead to

$$\begin{aligned}
 \dot{V} &= \dot{V}_2 + \frac{1}{\mu} \tilde{\boldsymbol{\theta}}^T \dot{\tilde{\boldsymbol{\theta}}} + \tilde{\mathbf{D}}(t)^T \left( \dot{\tilde{\mathbf{D}}}(t) - \mathbf{J} \tilde{\mathbf{D}}(t) \right) + \lambda_1^T \dot{\lambda}_1 + \lambda_2^T \dot{\lambda}_2 \\
 &\leq -\mathbf{e}_1^T \mathbf{K}_1 \mathbf{e}_1 - \mathbf{e}_2^T \mathbf{K}_2 \mathbf{e}_2 - \sum_{j=1}^n |e_{2j}| \|\lambda_{2j}\| \left\| \bar{\mathbf{M}}^{-1} \right\|^2 \mu \tilde{\boldsymbol{\theta}} + \frac{1}{\mu} \tilde{\boldsymbol{\theta}}^T \dot{\tilde{\boldsymbol{\theta}}} \\
 &\quad - \tilde{\mathbf{D}}(t)^T \mathbf{J} \tilde{\mathbf{D}}(t) + \tilde{\mathbf{D}}(t)^T \dot{\tilde{\mathbf{D}}}(t) + \lambda_1^T (-p_1 \lambda_1 + \lambda_2) \\
 &\quad + \lambda_2^T \left( \bar{\mathbf{M}}^{-1} (-p_2 \lambda_2 + \Delta \boldsymbol{\tau}) - \lambda_2 \left\| \bar{\mathbf{M}}^{-1} \right\|^2 \|\Delta \boldsymbol{\tau}\|^2 \right)
 \end{aligned} \tag{36}$$

According to Eq. (36), the adaptive update law of  $\hat{\boldsymbol{\theta}}$  is developed as:

$$\dot{\hat{\boldsymbol{\theta}}} = \mu \left( \mu |e_2| \left\| \bar{\mathbf{M}}^{-1} \right\|^2 \lambda_2 - \beta \hat{\boldsymbol{\theta}} \right) \tag{37}$$

where  $\beta > 0$  is the adaptive gain.

Substituting Eq. (37) into Eq. (36) yields

$$\begin{aligned}
 \dot{V} &\leq -\mathbf{e}_1^T \mathbf{K}_1 \mathbf{e}_1 - \mathbf{e}_2^T \mathbf{K}_2 \mathbf{e}_2 - \beta \left( \left( \hat{\boldsymbol{\theta}} - \boldsymbol{\theta} \right)^2 - \boldsymbol{\theta}^2 \right) - \tilde{\mathbf{D}}(t)^T \mathbf{J} \tilde{\mathbf{D}}(t) + \frac{1}{2} \tilde{\mathbf{D}}(t)^T \tilde{\mathbf{D}}(t) \\
 &\quad + \frac{1}{2} \dot{\tilde{\mathbf{D}}}(t)^T \dot{\tilde{\mathbf{D}}}(t) - \lambda_1^T p_1 \lambda_1 + \lambda_1^T \lambda_2 - \lambda_2^T \bar{\mathbf{M}}^{-1} p_2 \lambda_2 \\
 &\quad + \lambda_2^T \bar{\mathbf{M}}^{-1} \Delta \boldsymbol{\tau} - \lambda_2^T \lambda_2 \left\| \bar{\mathbf{M}}^{-1} \right\|^2 \|\Delta \boldsymbol{\tau}\|^2 \\
 &\leq -\mathbf{e}_1^T \mathbf{K}_1 \mathbf{e}_1 - \mathbf{e}_2^T \mathbf{K}_2 \mathbf{e}_2 - \lambda_1^T \left( p_1 - \frac{\mathbf{I}}{2} \right) \lambda_1 - \lambda_2^T \left( \bar{\mathbf{M}}^{-1} p_2 + \left\| \bar{\mathbf{M}}^{-1} \right\|^2 \|\Delta \boldsymbol{\tau}\|^2 - \mathbf{I} \right) \lambda_2 \\
 &\quad - \beta \tilde{\boldsymbol{\theta}}^2 - \lambda_{\min} \left( \mathbf{J} - \frac{\mathbf{I}}{2} \right) \tilde{\mathbf{D}}(t)^T \tilde{\mathbf{D}}(t) + \beta \boldsymbol{\theta}^2 + \frac{1}{2} \vartheta_3^2 \\
 &\quad + \frac{1}{2} \left\| \bar{\mathbf{M}}^{-1} \right\|^2 \|\Delta \boldsymbol{\tau}\|^2 \\
 &\leq -N V + \Psi
 \end{aligned} \tag{38}$$



where

$$N = \min \left\{ 2\lambda_{\min}(\mathbf{K}_1), 2\lambda_{\min}(\mathbf{K}_2), \lambda_{\min}(2\mathbf{p}_1 - \mathbf{I}), \right. \\ \left. 2\lambda_{\min} \left( \bar{\mathbf{M}}^{-1} \mathbf{p}_2 + \left\| \bar{\mathbf{M}}^{-1} \right\|^2 \|\Delta \boldsymbol{\tau}\|^2 - \mathbf{I} \right), \right. \\ \left. 2\lambda_{\min}(\beta), 2\lambda_{\min} \left( \mathbf{J} - \frac{\mathbf{I}}{2} \right) \right\} \tag{39}$$

$$\Psi = \beta \theta^2 + \frac{1}{2} \vartheta_3^2 + \frac{1}{2} \left\| \bar{\mathbf{M}}^{-1} \right\|^2 \|\Delta \boldsymbol{\tau}\|^2 > 0 \tag{40}$$

The parameters  $\mathbf{p}_1, \mathbf{p}_2$ , and  $\mathbf{J}$  need to be chosen in such way that the following conditions are satisfied

$$\lambda_{\min}(2\mathbf{p}_1 - \mathbf{I}) > 0, \lambda_{\min}(\bar{\mathbf{M}}^{-1} \mathbf{p}_2 + \left\| \bar{\mathbf{M}}^{-1} \right\|^2 \|\Delta \boldsymbol{\tau}\|^2 - \mathbf{I}) > 0, \lambda_{\min} \left( \mathbf{J} - \frac{\mathbf{I}}{2} \right) > 0 \tag{41}$$

From Eqs. (38)–(41), we have

$$0 \leq V \leq \frac{\Psi}{N} + \left( V(0) - \frac{\Psi}{N} \right) e^{-Nt} \tag{42}$$

From Lemma 4 and Eq. (42), it follows that  $V$  is bounded when  $t \rightarrow \infty, V = \frac{\Psi}{N}$ . Thus,  $\mathbf{e}_1, \mathbf{e}_2, \tilde{\boldsymbol{\theta}}, \tilde{\mathbf{D}}(t), \boldsymbol{\lambda}_1$  and  $\boldsymbol{\lambda}_2$  in the system are uniformly ultimately bounded. Since  $\mathbf{e}_1$  and  $\boldsymbol{\lambda}_1$  are bounded, and  $\mathbf{e}_1 = \mathbf{x}_1 - \mathbf{y}_d - \boldsymbol{\lambda}_1$  in Eq. (21), the position tracking error  $\mathbf{x}_1 - \mathbf{y}_d$  is uniformly ultimately bounded.

However,  $\text{sign}(\bullet)$  function may lead to chattering phenomenon. In order to obtain good linear characteristics,  $\text{sign}(\bullet)$  is replaced by a smoother function  $\text{tansig}(\bullet)$ . Furthermore, a parameter  $\sigma$  is introduced to adjust the width of the approximate linear band. The smaller the  $\sigma$  is, the wider the width of the approximate linear band is. The function is as follows:

$$\text{tansig}(\sigma \cdot) = \frac{2}{1 + e^{(-2\sigma \cdot)}} - 1 \tag{43}$$

Finally, the model-free adaptive robust controller can be written as:

$$\boldsymbol{\tau} = \underbrace{\mathbf{u}_{t-L} - \bar{\mathbf{M}} \left( \dot{\mathbf{x}}_{2(t-L)} + \hat{\mathbf{D}}(t) \right)}_{\text{TDE + TDE error observer}} + \underbrace{\bar{\mathbf{M}} (-\mathbf{K}_2 \mathbf{e}_2 - \mathbf{e}_1 + \dot{\boldsymbol{\alpha}})}_{\text{robust terms}} \\ + \underbrace{\mu \kappa \left\| \bar{\mathbf{M}}^{-1} \right\|^2 \boldsymbol{\lambda}_2 \hat{\boldsymbol{\theta}}}_{\text{input saturation compensate terms}} - \mathbf{p}_2 \boldsymbol{\lambda}_2 \tag{44}$$

where  $\kappa = \text{diag}[\text{tansig}(\sigma \mathbf{e}_{2i})]$ .

**Remark 2.** Compared with the basic simple controllers such as MPC and Proportional-Derivative (PD), our proposed model-free adaptive robust controller can deal with disturbance and input saturation simultaneously. Meanwhile, it does not necessitate the accurate dynamic model of the complicated system.

### 5. Simulation studies

In order to verify the effectiveness of the method in this paper, a two-link robot as shown in Fig. 2 is used. The mathematical model of the two-link robot is given as follows [43]:

$$\begin{aligned}
 \mathbf{M}(\mathbf{q}) &= \begin{bmatrix} (m_1 + m_2) r_1^2 + m_2 r_2^2 + 2m_2 r_1 r_2 \cos(q_2) & m_2 r_2^2 + m_2 r_1 r_2 \cos(q_2) \\ m_2 r_2^2 + m_2 r_1 r_2 \cos(q_2) & m_2 r_2^2 \end{bmatrix} \\
 \mathbf{C}(\mathbf{q}, \dot{\mathbf{q}}) &= \begin{bmatrix} -m_2 r_1 r_2 \sin(q_2) \dot{q}_2 & -m_2 r_1 r_2 \sin(q_2) (\dot{q}_1 + \dot{q}_2) \\ m_2 r_1 r_2 \sin(q_2) \dot{q}_1 & 0 \end{bmatrix} \\
 \mathbf{G}(\mathbf{q}) &= \begin{bmatrix} (m_1 + m_2) r_1^2 \cos(q_2) g + m_2 r_2 \cos(q_1 + q_2) g \\ m_2 r_2 \cos(q_1 + q_2) g \end{bmatrix} \tag{45}
 \end{aligned}$$

In the simulation, parameters of the two-link robot are shown in Table I. The input saturation is  $\begin{cases} \tau_{\max} = 15 \\ \tau_{\min} = -16 \end{cases}$ . The friction is assumed to be  $\mathbf{F}(\dot{\mathbf{q}}) = \begin{bmatrix} 0.02 \sin(q_1) \\ 0.02 \sin(q_2) \end{bmatrix}$ , and the external disturbance is  $\mathbf{d} = 2 \times \begin{bmatrix} 2.5 \sin(2\Pi t) + 4 \sin(3\Pi) + 1.3 \\ 5 \sin(2\Pi t - \Pi/2) + 0.6 \sin(5\Pi t) + 1.4 \end{bmatrix}$ .

The desired trajectory is given as  $\mathbf{y}_d = \begin{bmatrix} y_{1d} \\ y_{2d} \end{bmatrix} = \begin{bmatrix} 0.4 \sin(\Pi t) + 0.4 \cos(\Pi t) \\ 0.6 \sin(\Pi t) + 0.6 \cos(\Pi t) \end{bmatrix}$ . The initial condition of the position, auxiliary system states, and the adaptive bounds are chosen as  $q_1(0) = q_2(0) = 0.55$ ,  $\lambda_1(0) = \lambda_2(0) = [0; 0]$ ,  $\theta_1(0) = \theta_2(0) = 0.01$ , respectively.

The control method proposed in this paper is compared with the methods in refs. [23] and [37]. Simulations are conducted with various feedback gains in two cases.

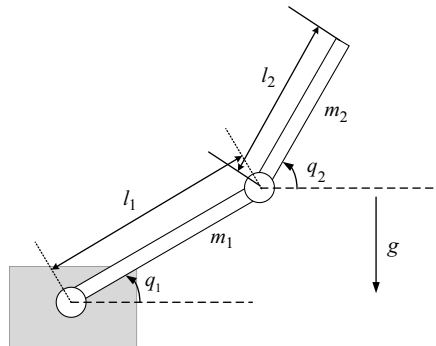


Figure 2. Model of a two-link robot.

Table I. Simulation parameters of the two-link robot.

Symbol	Definition	Value
$r_1$	Length of link 1	0.38 m
$r_2$	Length of link 2	0.31 m
$m_1$	Mass of link 1	2 kg
$m_2$	Mass of link 2	0.85 kg
$g$	Gravity acceleration	9.8 m/s <sup>2</sup>

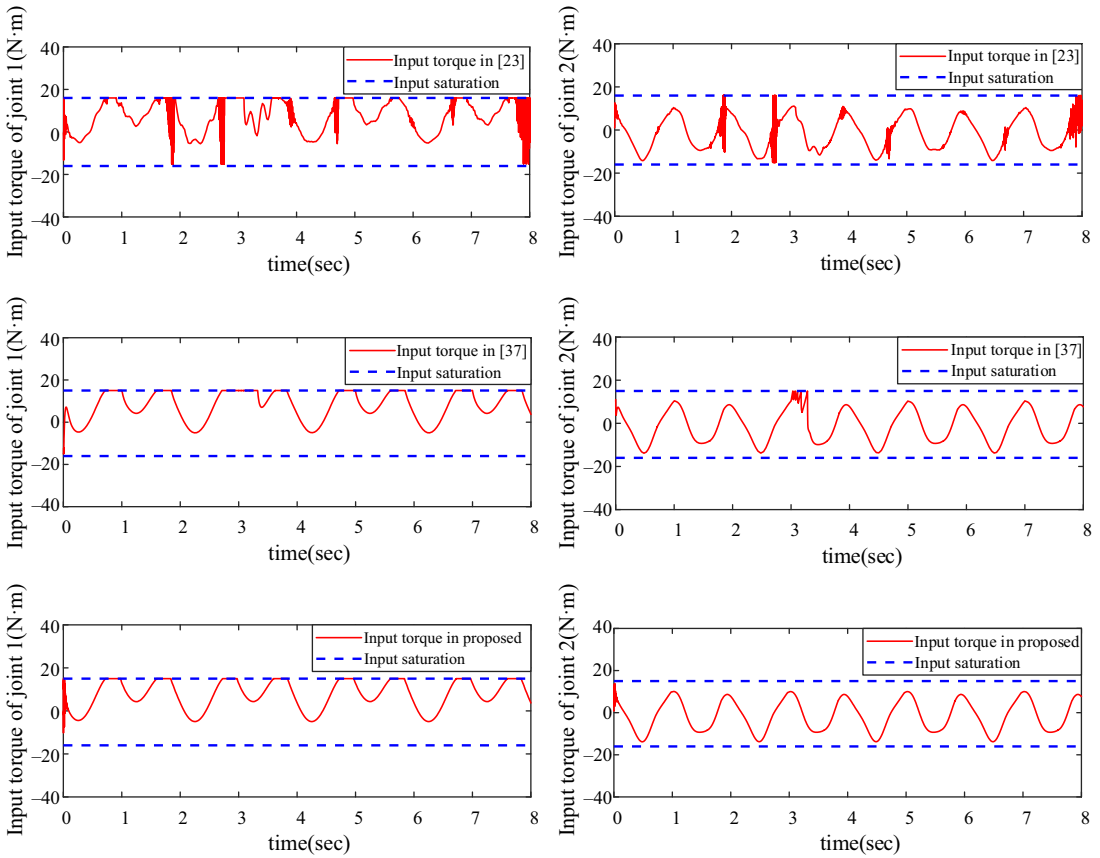


Figure 3. Control input signals.

5.1. Case 1. With larger gain

In case 1, the parameters in the proposed method are  $K_1 = [2\ 0; 0\ 2]$ ,  $K_2 = [20\ 0; 0\ 20]$ ,  $p_1 = [2\ 0; 0\ 2]$ ,  $p_2 = [260\ 0; 0\ 260]$ ,  $J = [440\ 0; 0\ 440]$ ,  $\bar{M} = [0.35\ 0; 0\ 0.05]$ ,  $\beta = 0.01$ ,  $\mu = 0.8$ , and  $\sigma = 20$ .

Figure 3 shows the control input signals in refs. [23, 37] and this paper. Since the input saturation cannot be handled in ref. [23], it can be seen that the method in ref. [23] generates severe chattering when the input torque reaches the saturation limit. In ref. [37], since an auxiliary system is developed to deal with the adverse effects of the input saturation limit, it can be seen that the input torque is smoother than that in ref. [23]; however, there is still chattering. The method proposed in this paper can compensate for the input saturation better by introducing the saturation deviation boundary to the auxiliary system and the adaptive law for it.

Figures 4 and 5 show the joint position tracking and position tracking errors. From Fig. 4, it can be seen that the method in ref. [23] becomes significantly worse in position tracking when the input saturation occurs. The position tracking performance in ref. [37] is improved compared with that in ref. [23] when input saturation occurs. The method proposed in this paper can track the desired position and does not result in large position error when the input saturation occurs. Figure 5 shows that the tracking error of the proposed method converges to zero quickly, and compared with the other two methods, the position tracking error is smaller. Furthermore, the proposed method can maintain desired tracking performance when the input saturation occurs due to the effective compensation of the input saturation.

Figures 6 and 7 show the TDE error observations and the adaptive results of the saturation deviation boundary developed in this paper. One can see that the value of  $\hat{\theta}$  of joint 1 is constantly adjusting when

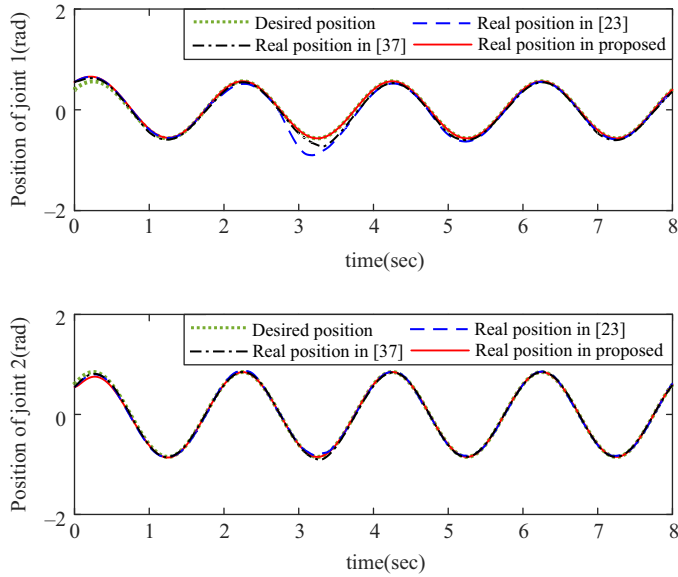


Figure 4. Position tracking.

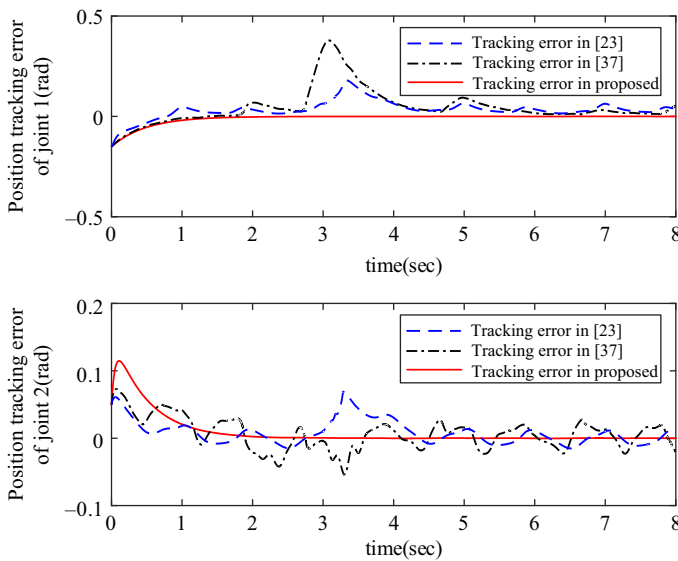
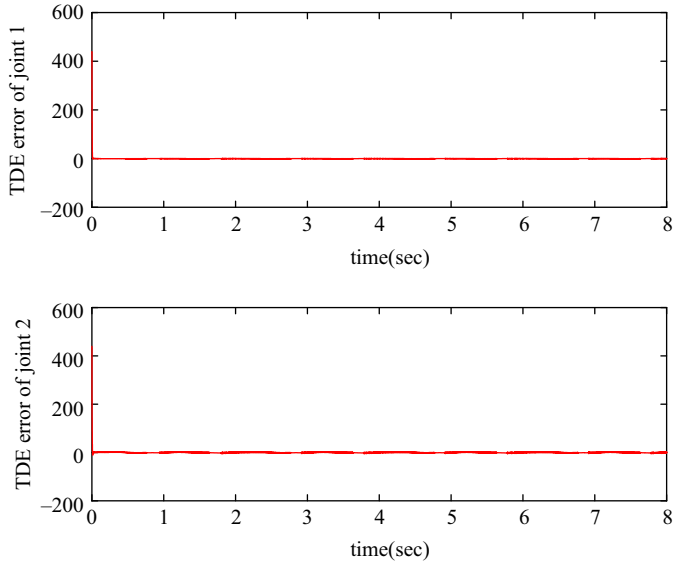


Figure 5. Position tracking errors.

the input saturation occurs, while the value of  $\hat{\theta}$  of joint 2 does not change because no input saturation occurs.

5.2. Case 2. With smaller gain

It can be seen from Case 1 that the chattering in the controller [23] is severe with a larger control gain. Now, a smaller feedback gain is taken in Case 2 where  $K_2 = [10\ 0; 0\ 10]$  and other comparison conditions are kept unchanged. The results are shown in Figs. 8–10.



**Figure 6.** TDE error observations in proposed method.

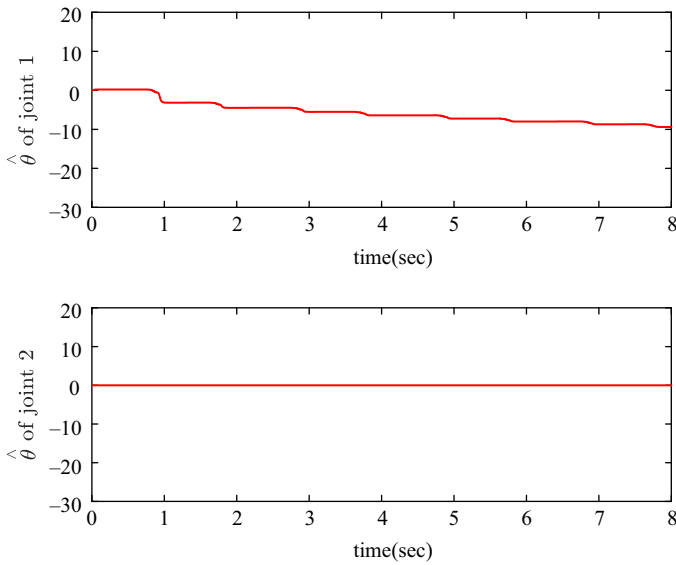


**Figure 7.** Adaptive saturation deviation boundary in proposed method.

In Fig. 8 with smaller feedback gain, the torque chattering in refs. [23] and [37] are reduced compared with Fig. 3 with larger gain. However, the reduction of chattering in refs. [23] and [37] is at the cost of larger tracking errors as shown in Figs. 9 and 10 compared with Figs. 4 and 5. In contrast to refs. [23] and [37], the torque in the proposed method still maintains smooth without severe chattering in Fig. 8. Meanwhile, the proposed method still achieves the optimal tracking accuracy among the three methods. Moreover, the saturation time of the proposed method is the least. Table II further shows the statistical analysis of the three methods. The index mean absolute percentage error (MAPE) is used to

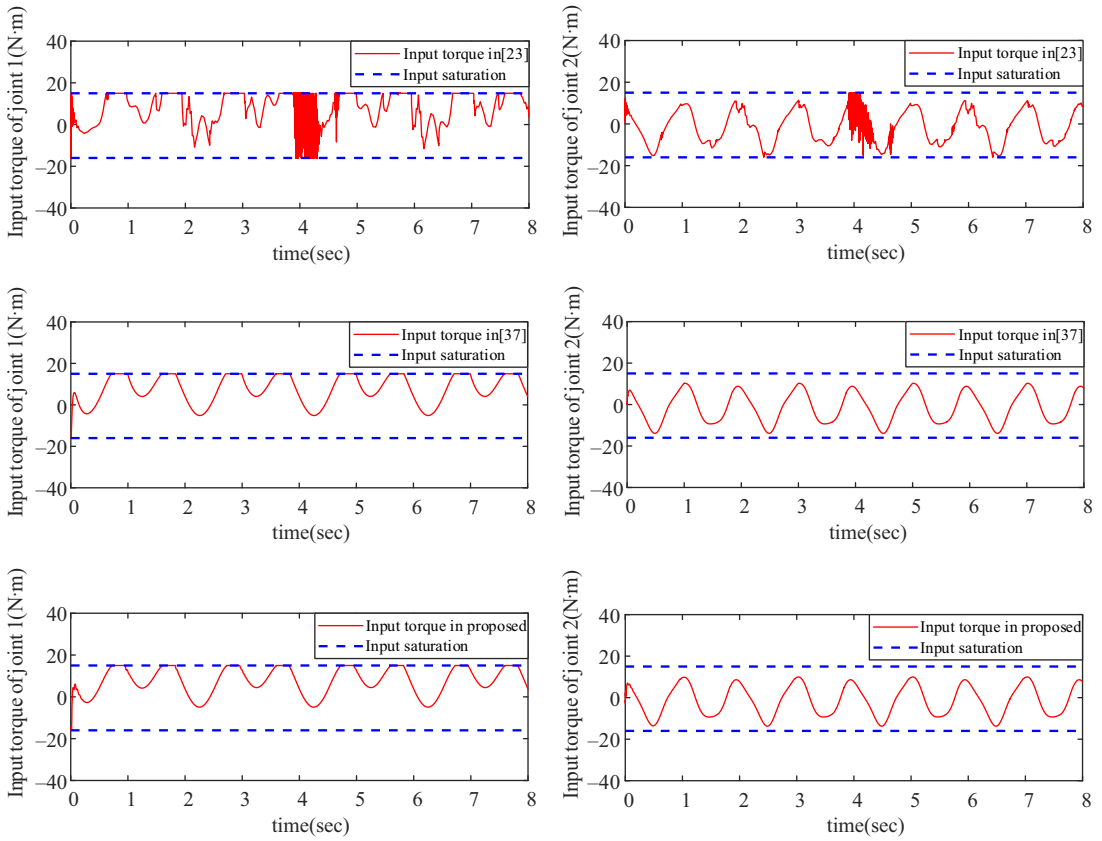


Figure 8. Control input signals.

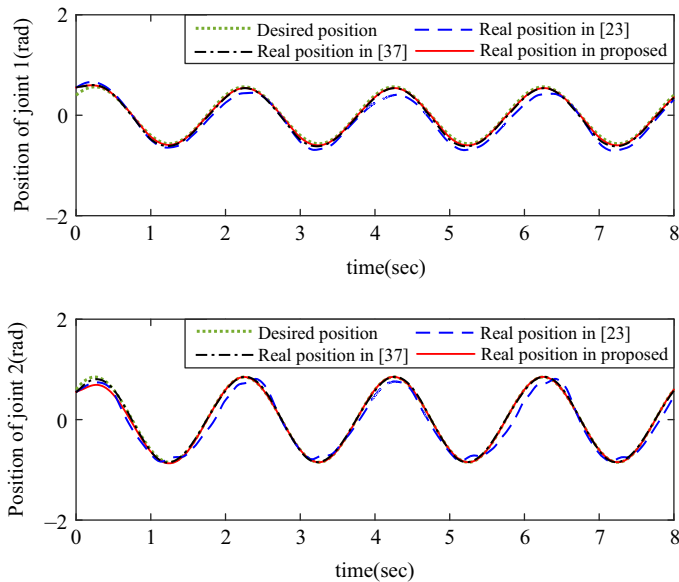


Figure 9. Position tracking.

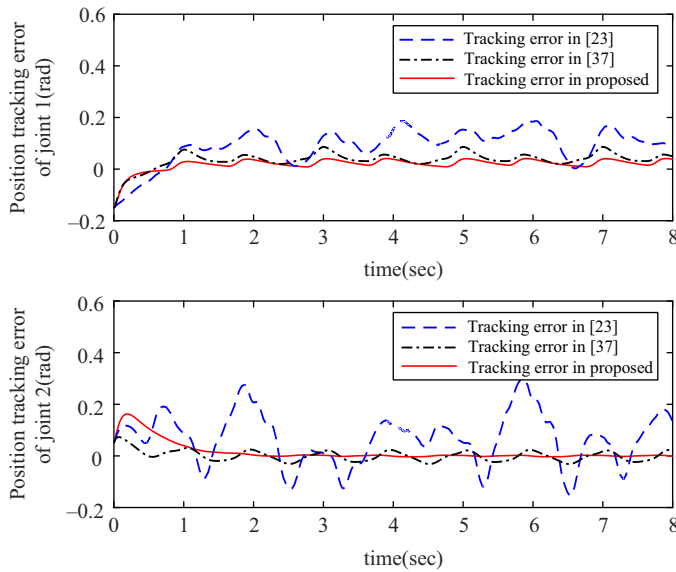


Figure 10. Position tracking errors.

Table II. Statistical analysis.

Gain	Method	Joint	Torque	Saturation time	MAPE of tracking errors
Larger gain	[23]	Joint 1	Severe chattering	2.0497 s	175.0475%
		Joint 2	Severe chattering	0.0083 s	25.9561%
	[37]	Joint 1	Small chattering	2.4472 s	40.8751%
		Joint 2	Small chattering	0.0000 s	5.7522%
	Proposed	Joint 1	Smooth	1.9732 s	13.9512%
		Joint 2	Smooth	0.0000 s	4.3447%
Smaller gain	[23]	Joint 1	Small chattering	3.0202 s	177.1326%
		Joint 2	Small chattering	0.0529 s	180.7400%
	[37]	Joint 1	Smooth	2.0404 s	60.5572%
		Joint 2	Smooth	0.0000 s	7.7787%
	Proposed	Joint 1	Smooth	1.7922 s	17.1934%
		Joint 2	Smooth	0.0000 s	6.7811%

evaluate the tracking errors, where  $MAPE = \frac{1}{\tilde{N}} \sum_{k=1}^{\tilde{N}} \left| \frac{y(k) - y_d(k)}{y_d(k)} \right| * 100\%$ ,  $k = 1, 2, \dots, \tilde{N}$  represents each sampling time.

### 6. Experiments

In this section, the experiments are conducted on a Phantom Omni robot. The experimental setup is composed of a Phantom Omni robot and a computer, which is shown in Fig. 11. The robot is connected to the computer through a 1394 FireWire cable. In the experiments, the first and third joints are used (the second joint is locked for brevity). In the experiments, the proposed method is also compared with the methods in refs. [23] and [37].

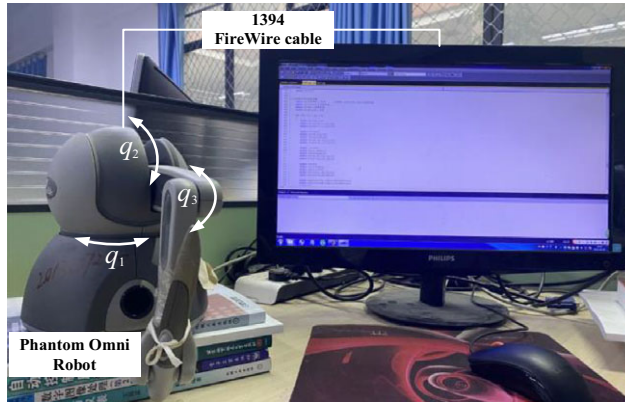


Figure 11. Experimental setup.

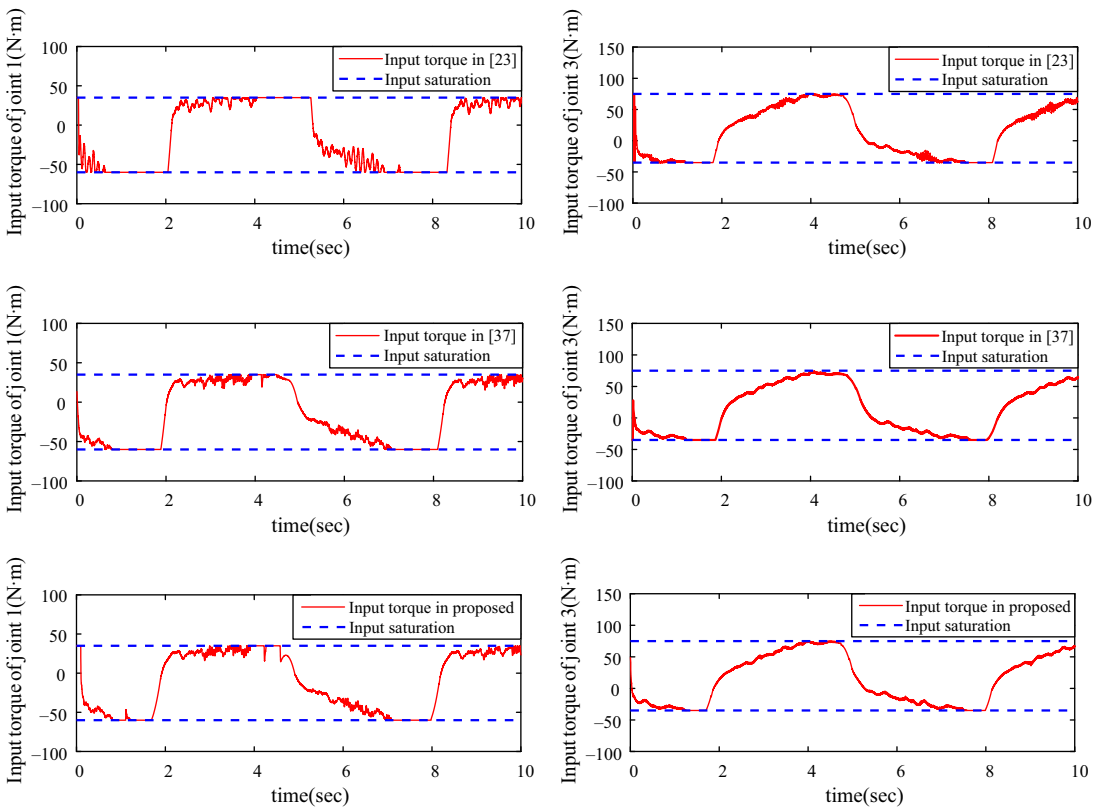


Figure 12. Control input signals.

The parameters of the controller are taken as  $\mathbf{K}_1 = [60 \ 0; 0 \ 60]$ ,  $\mathbf{K}_2 = [100 \ 0; 0 \ 100]$ ,  $\mathbf{p}_1 = [60 \ 0; 0 \ 60]$ ,  $\mathbf{p}_2 = [200 \ 0; 0 \ 200]$ ,  $\mathbf{J} = [140 \ 0; 0 \ 140]$ ,  $\bar{\mathbf{M}} = [0.5 \ 0; 0 \ 0.9]$ ,  $\beta = 0.02$ ,  $\mu = 0.6$ ,  $\sigma = 40$ . The disturbance is  $\mathbf{d} = \begin{bmatrix} 3 \sin(2t + 0.785) \\ 3 \sin(2t + 0.785) \end{bmatrix}$ , and the desired trajectory is given as  $\mathbf{q}_d = \begin{bmatrix} q_{1d} \\ q_{3d} \end{bmatrix} = \begin{bmatrix} 0.4 \sin(\Pi t) + 0.4 \cos(\Pi t) \\ 0.6 \sin(\Pi t) + 0.6 \cos(\Pi t) \end{bmatrix}$ . The input saturation for joint 1 and joint 3 are set as  $\begin{cases} \tau_{1 \max} = 35 \\ \tau_{1 \min} = -60 \end{cases}$ , and  $\begin{cases} \tau_{3 \max} = 75 \\ \tau_{3 \min} = -35 \end{cases}$ .



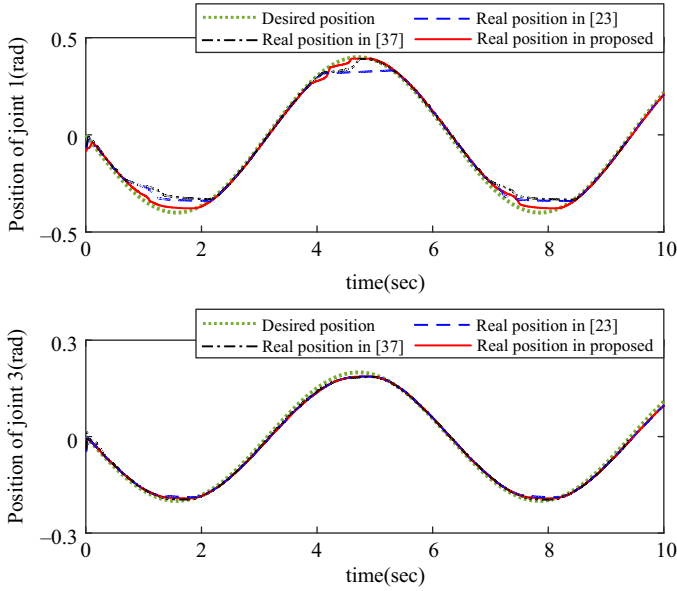


Figure 13. Position tracking.

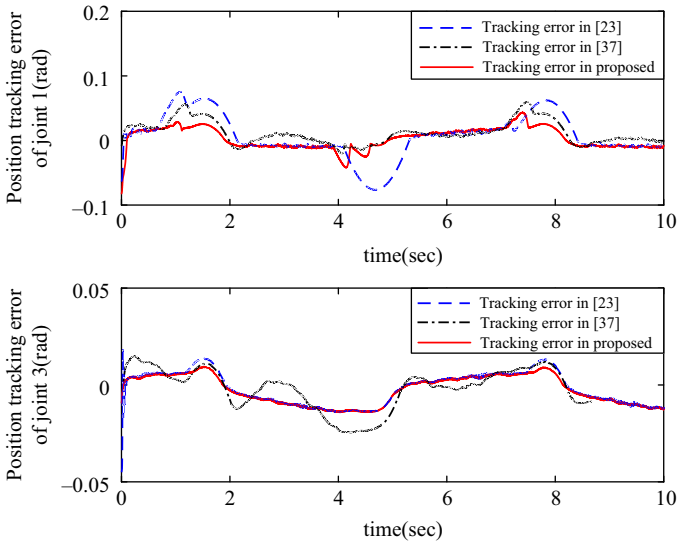
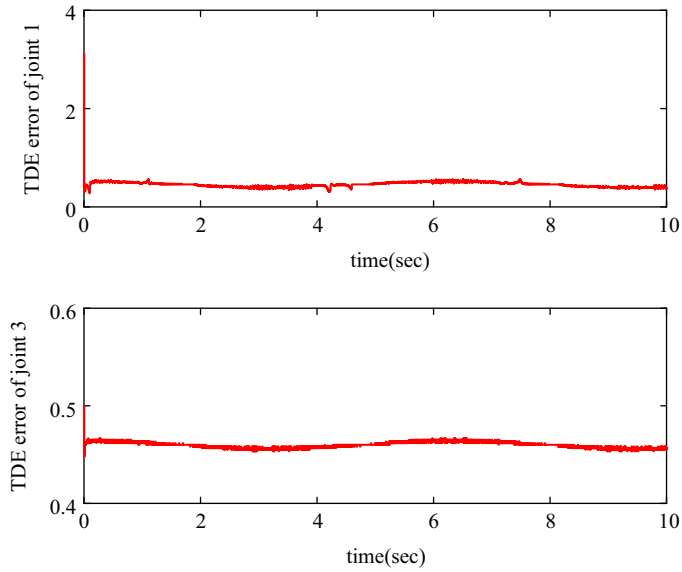
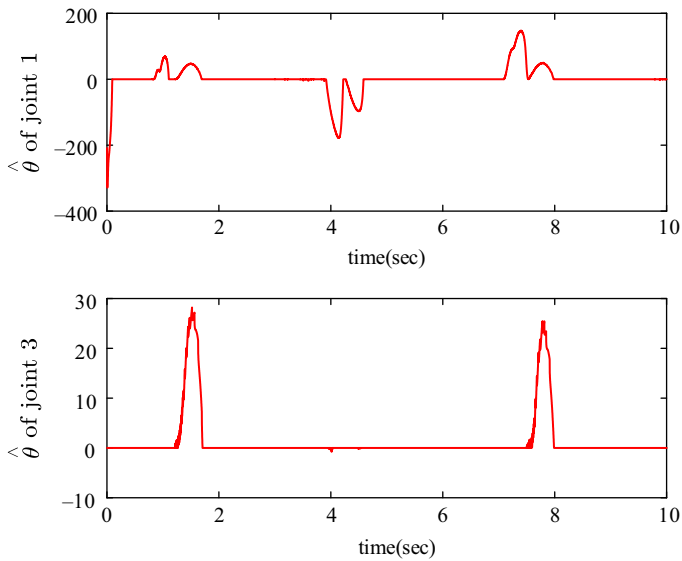


Figure 14. Position tracking errors.

Figures 12–16 show the experimental results of the methods in refs. [23, 37] and the proposed method. The proposed method takes the TDE error and input saturation into account compared with ref. [23]. The saturation deviation boundary is introduced based on the auxiliary system in ref. [37] to further attenuate the negative impact of input saturation on the system. Comparing with Figs. 12–14, we can see that the proposed method can adequately cope with the effect of input saturation on position tracking when input saturation occurs and achieve accurate tracking. The control performance in the proposed method is better than those in refs. [23] and [37]. The time and the position error when input saturation occurs are significantly less than those of the other two methods. The TDE error observation and the adaptive saturation deviation boundary are shown in Figs. 15 and 16.



**Figure 15.** TDE error observation in proposed method.



**Figure 16.** Adaptive saturation deviation boundary in proposed method.

In summary, the control method proposed in this paper achieves desired position tracking for robotic system with external disturbances under input saturation. It can effectively reduce the position tracking error and saturation time caused by input saturation without computing the complicated dynamics model of the robot.

### 7. Conclusions

This paper proposes a model-free adaptive robust control based on TDE for robot with disturbance and input saturation. TDE is adopted to estimate all the uncertainty terms and external disturbance under

input saturation of the system. The TDE error observer is used to estimate the approximation errors of the nonlinear terms. The adaptive auxiliary system is developed to reduce the undesirable effects of the input saturation. The backstepping is employed to obtain the final model-free adaptive robust controller. This method does not necessitate the accurate dynamic model of the complicated system while guaranteeing the desired position tracking performance of the robot even subject to disturbance and input saturation. The validity of the proposed method is demonstrated by both simulations and experiments. Besides, fault-tolerant control for resilient robot is an interesting topic and a significant challenge [44, 45]. Therefore, how to extend our proposed method to deal with faults, disturbance, and input saturation simultaneously to ensure a safe and effective control for resilient robot needs to be further investigated.

**Author contributions.** Xia Liu: conceptualization (lead), review, and editing (lead), original draft (lead), funding acquisition (lead); Lu Wang: review and editing (equal), investigation (equal), software (equal); and Yong Yang: conceptualization (supporting); software (equal), and funding acquisition (equal).

**Financial support.** This work is supported by the National Natural Science Foundation of China under Grants 61973257 and 62003278, and the Natural Science Foundation of Sichuan Province under Grants 2023NSFSC0510 and 2023NSFSC1431.

**Competing interests.** The authors declare that they have no known competing financial interests or personal relationships that could have appeared to influence the work reported in this paper.

**Ethical approval.** Not applicable.

## References

- [1] J.-Y. Long, J.-D. Mou, L.-W. Zhang, S.-H. Zhang and C. Li, "Attitude data-based deep hybrid learning architecture for intelligent fault diagnosis of multi-joint industrial robots," *J. Manuf. Syst.* **61**, 736–745 (2021).
- [2] R. Zhao, M.-Z. Miao, J.-M. Lu, Y. Wang and D.-L. Li, "Formation control of multiple underwater robots based on ADMM distributed model predictive control," *Ocean Eng.* **257**, 1–14 (2022).
- [3] Y.-Q. Wang, J.-J. Cao, R.-R. Geng, L. Zhou and L. Wang, "Study on the design and control method of a wire-driven waist rehabilitation training parallel robot," *Robotica* **40**(10), 3499–3513 (2022).
- [4] L. Cheng, Z.-G. Huo, M. Tan and W. J. Zhang, "Tracking control of a closed-chain five-bar robot with two degrees of freedom by integration of an approximation-based approach and mechanical design," *IEEE Trans. Syst. Man Cybern. Part B Cybern.* **42**(5), 1470–1479 (2021).
- [5] M.-C. Pai, "Adaptive observer-based global sliding mode control for uncertain discrete-time nonlinear systems with time-delays and input nonlinearity," *Asian J. Control* **21**(5), 2290–2300 (2019).
- [6] A. Ferrara, G. P. Incremona and B. Sangiovanni, "Tracking control via switched Integral Sliding Mode with application to robot manipulators," *Control Eng. Pract.* **90**, 257–266 (2019).
- [7] M. Naserian, A. Ramazani, A. Khaki-Sedigh and A. Moarefianpour, "Fast terminal sliding mode control for a nonlinear multi-agent robot system with disturbance," *Syst. Sci. Control. Eng.* **8**(1), 328–338 (2020).
- [8] N. F. Silva, C. E. T. Dórea and A. L. Maitell, "An iterative model predictive control algorithm for constrained nonlinear systems," *Asian J. Control* **21**(5), 2193–2207 (2019).
- [9] Y. Chen, Z.-J. Li, H.-Y. Kong and F. Ke, "Model predictive tracking control of nonholonomic mobile robots with coupled input constraints and unknown dynamics," *IEEE Trans. Industr. Inform.* **15**(6), 3196–3205 (2019).
- [10] A. Carron, E. Arcari, M. Wermelinger, L. Hewing, M. Hutter and M. N. Zeilinger, "Data-driven model predictive control for trajectory tracking with a robotic arm," *IEEE Robot. Autom. Lett.* **4**(4), 3758–3765 (2019).
- [11] X.-J. Li and X.-Y. Shen, "A data-driven attack detection approach for DC servo motor systems based on mixed optimization strategy," *IEEE Trans. Industr. Inform.* **16**(9), 5806–5813 (2020).
- [12] J.-F. Wang, H. Dong, F.-H. Chen, M. T. Vu, A. D. Shakibjoo and A. Mohammadzadeh, "Formation control of non-holonomic mobile robots: Predictive data-driven fuzzy compensator," *Mathematics* **11**(8), 1–21 (2023).
- [13] H.-Y. Huang, H. Xu, F.-H. Chen, C.-W. Zhang and A. Mohammadzadeh, "An applied type-3 fuzzy logic system: Practical Matlab Simulink and M-files for robotic, control, and modeling applications," *Symmetry* **15**(2), 1–16 (2023).
- [14] S. Ding, J.-Z. Peng, H. Zhang and Y.-N. Wang, "Neural network-based adaptive hybrid impedance control for electrically driven flexible-joint robotic manipulators with input saturation," *Neurocomputing* **458**, 99–111 (2021).
- [15] Y.-Q. Wu and R.-Q. Lu, "Output synchronization and L2-gain analysis for network systems," *IEEE Trans. Syst. Man Cybern. Syst.* **48**(2), 2105–2114 (2018).
- [16] Y.-X. Wu, R. Huang, X. Li and S. Liu, "Adaptive neural network control of uncertain robotic manipulators with external disturbance and time-varying output constraints," *Neurocomputing* **323**(5), 108–116 (2019).

- [17] G.-R. Lin, B.-Q. Shan, Y.-M. Ma, X.-C. Tian and J.-P. Yu, “Adaptive neural network command filtered backstepping impedance control for uncertain robotic manipulators with disturbance observer,” *Trans. Inst. Meas. Control* **44**(4), 799–808 (2021).
- [18] P.-R. Ouyang, W.-J. Zhang and M. M. Gupta, “An adaptive switching learning control method for trajectory tracking of robot manipulators,” *Mechatronics* **16**(1), 51–61 (2006).
- [19] M.-H. Li, R. J. Kang, D. T. Branson and J. S. Dai, “Model-free control for continuum robots based on an adaptive Kalman Filter,” *IEEE-ASME Trans. Mechatron.* **23**(1), 286–297 (2018).
- [20] K. Youcef-Toumi and O. Ito, “A Time Delay Controller for Systems with Unknown Dynamics,” *In: 1988 American Control Conference* (1988) pp. 133–142.
- [21] S. Ahmed, H.-P. Wang and Y. Tian, “Adaptive High-Order terminal sliding mode control based on time delay estimation for the robotic manipulators with backlash hysteresis,” *IEEE Trans. Syst. Man Cybern. Syst.* **51**(2), 1128–1137 (2019).
- [22] S. Roy, S. Baldi, P. Li and V. N. Sankaranarayanan, “Artificial-delay adaptive control for underactuated Euler-Lagrange robotics,” *IEEE-ASME Trans. Mechatron.* **26**(6), 3064–3075 (2021).
- [23] B. Brahmi, M. Saad, C. Ochoa-Luna, M. H. Rahman and A. Brahmi, “Adaptive tracking control of an exoskeleton robot with uncertain dynamics based on estimated time-delay control,” *IEEE-ASME Trans. Mechatron.* **23**(2), 575–585 (2018).
- [24] S. Roy, J. Lee and S. Baldi, “A new adaptive-robust design for time delay control under state-dependent stability condition,” *IEEE Trans. Control Syst. Technol.* **29**(1), 420–427 (2021).
- [25] H.-Z. Wang, L.-J. Fang, T.-Z. Song, J.-Q. Xu and H.-S. Shen, “Model-free adaptive sliding mode control with adjustable funnel boundary for robot manipulators with uncertainties,” *Rev. Sci. Instrum.* **92**(6), 1–11 (2021).
- [26] J. Lee, P. H. Chang and M.-L. Jin, “Adaptive integral sliding mode control with time-delay estimation for robot manipulators,” *IEEE Trans. Ind. Electron.* **64**(8), 6796–6804 (2017).
- [27] Y.-Y. Wang, L.-F. Liu, D. Wang, F. Ju and B. Chen, “Time-delay control using a novel nonlinear adaptive law for accurate trajectory tracking of Cable-Driven Robots,” *IEEE Trans. Ind. Inform.* **16**(8), 5234–5243 (2019).
- [28] T.-Z. Song, L.-J. Fang and H.-Z. Wang, “Model-free finite-time terminal sliding mode control with a novel adaptive sliding mode observer of uncertain robot systems,” *Asian J. Control* **24**(3), 1437–1451 (2021).
- [29] C.-G. Yang, D.-Y. Huang, W. He and L. Cheng, “Neural control of robot manipulators with trajectory tracking constraints and input saturation,” *IEEE Trans. Neural Netw. Learn. Syst.* **32**(9), 4231–4242 (2020).
- [30] M.-Y. Ye, G.-Q. Gao, J.-W. Zhong and Q.-Y. Qin, “Finite-time dynamic tracking control of parallel robots with uncertainties and input saturation,” *Sensors* **21**(9), 1–18 (2021).
- [31] Y.-C. Sun, X.-Y. Chen, Z.-W. Wang, H.-D. Qin and R.-J. Jing, “Adaptive interval type-2 fuzzy control for multi-legged underwater robot with input saturation and full-state constraints,” *Int. J. Syst. Sci.* **3**, 1–16 (2021). doi: [10.1080/00207721.2020.1869346](https://doi.org/10.1080/00207721.2020.1869346).
- [32] S.-Y. Jia and J.-J. Shan, “Finite-time trajectory tracking control of space manipulator under actuator saturation,” *IEEE Trans. Ind. Electron.* **67**(3), 2086–2096 (2020).
- [33] Y.-S. Hu, H.-C. Yan, H. Zhang, M. Wang and L. Zeng, “Robust adaptive fixed-time sliding-mode control for uncertain robotic systems with input saturation,” *IEEE Trans. Cybern.* **53**(4), 2636–2646 (2022). doi: [10.1109/TCYB.2022.3164739](https://doi.org/10.1109/TCYB.2022.3164739).
- [34] Y. Yang, J. Tan and D. Yue, “Prescribed performance control of One-DOF link manipulator with uncertainties and input saturation constraint,” *IEEE-CAA J. Automat. Sin.* **6**(1), 148–157 (2018).
- [35] R.-Y. Jin, P. Rocco, X. Q. Chen and Y.-H. Geng, “LPV-based offline model predictive control for free-floating space robots,” *IEEE Trans. Aerosp. Electron. Syst.* **57**(6), 3896–3904 (2021).
- [36] T. Zhou, Y.-G. Xu and B. Wu, “Smooth fractional order sliding mode controller for spherical robots with input saturation,” *Appl. Sci. Basel* **10**(6), 1–17 (2020).
- [37] X. Hu, X.-J. Wei, H.-F. Zhang, J. Han and X.-H. Liu, “Robust adaptive tracking control for a class of mechanical systems with unknown disturbances under actuator saturation,” *Int. J. Robust Nonlinear Control* **29**(6), 1893–1908 (2019).
- [38] M. Jin, J. Lee and N. G. Tsagarakis, “Model-free robust adaptive control of humanoid robots with flexible joints,” *IEEE Trans. Ind. Electron.* **64**(2), 1706–1715 (2017).
- [39] J. Baek and H. Baek, “A time-delayed control scheme using adaptive law with time-varying boundedness for robot manipulators,” *Appl. Sci. Basel* **10**(1), 1–17 (2019).
- [40] Z.-J. Li, C.-Y. Su, L.-Y. Wang, Z.-T. Chen and T.-Y. Chai, “Nonlinear disturbance observer-based control design for a robotic exoskeleton incorporating fuzzy approximation,” *IEEE Trans. Ind. Electron.* **62**(9), 5763–5775 (2015).
- [41] M. Sababheh and D. Choi, “A complete refinement of young’s inequality,” *J. Math. Anal. Appl.* **440**(1), 379–393 (2016).
- [42] W. He, Y.-T. Dong and C.-Y. Sun, “Adaptive neural impedance control of a robotic manipulator with input saturation,” *IEEE Trans. Syst. Man Cybern. Syst.* **46**(3), 334–344 (2016).
- [43] J. Baek, S. Cho and S. Han, “Practical time-delay control with adaptive gains for trajectory tracking of robot manipulators,” *IEEE Trans. Ind. Electron.* **65**(7), 5682–5692 (2018).
- [44] F. Wang, Z.-Q. Qian, Z.-G. Yan, C.-W. Yuan and W.-J. Zhang, “A novel resilient robot: Kinematic analysis and experimentation,” *IEEE Access* **8**, 2885–2892 (2020).
- [45] T. Zhang, W.-J. Zhang and M. M. Gupta, “Resilient robots: Concept, review, and future directions,” *Robotics* **6**(4), 1–14 (2017).